Semiconductor Physics, Quantum Electronics & Optoelectronics, 2023. V. 26, No 1. P. 076-083.

Optics

Optical characteristics of silver-based nanocomposites fabricated by an environmentally friendly method

T.O. Malakhovska[1], **A.I. Pogodin**[1], **M.J. Filep**[1,2], **M.M. Pop**[1], **Ya.I. Studenyak**[1], **K.M. Nemesh**[1], **R. Mariychuk**[3], **V.V. Vakulchak**[1], **V. Komanicky**[4], **S. Vorobiov**[4]

[1]*Uzhhorod National University, 46, Pidhirna str., 88000 Uzhhorod, Ukraine*
[2]*Ferenc Rakoczi II Transcarpathian Hungarian College of Higher Education, Kossuth Sq. 6, 90200 Beregovo, Ukraine*
[3]*University of Presov, Faculty of Humanity and Natural Sciences, Department of Ecology,*
17th November 1, Presov 08116, Slovakia
[4]*P.J. Šafarik University, Institute of Physics, Faculty of Science, Park Angelinum 9, 04154 Kosice, Slovakia*
**Corresponding author e-mail: t.malakhovska@gmail.com*

Abstract. This work presents a simple and environmentally friendly method of synthesis of chitosan and Ag nanocomposites. The structure of the obtained organic matrix was determined by Fourier-transform infrared spectroscopy (FTIR). Formation of chitosan-chitin copolymer was discovered. Nanocomposite films with silver content of 9–71 wt.% were prepared. The microstructure and elemental composition of the obtained films were investigated by scanning electron microscopy (SEM) and energy dispersive X-ray spectroscopy (EDS). The prepared films are characterized by uniform distribution of silver nanoparticles in the organic matrix. Optical properties were studied by diffuse reflectance spectroscopy. The diffuse reflectance spectra of the films have maxima. The increase of the Ag^0 concentration in the nanocomposite films was found to lead to the maximum shift of the diffuse reflectance spectra to longer wavelengths. The optical transitions energies were estimated using the Kubelka–Munk function in combination with the Tauc method.

Keywords: chitosan, nanoparticles, composites, scanning electron microscopy, diffuse reflectance spectroscopy.

https://doi.org/10.15407/spqeo26.01.076
PACS 61.82.Rx, 68.37.Hk, 72.80.Tm

Manuscript received 04.01.23; revised version received 06.02.23; accepted for publication 08.03.23; published online 24.03.23.

1. Introduction

Due to the rapid progress in miniaturization, autonomy and stability of electronic devices, considerable attention is paid to the research on application of nanoparticles [1]. Nanoparticles are a link between the bulk materials and the molecular or atomic structures [1, 2]. Moreover, properties of nanoparticles may significantly differ from those of bulk materials. Numerous studies of nanoparticles deal with great variability of their properties defined by both their sizes and morphology [3, 4]. Nanomaterials have large-scale application from consumer goods to energy-saving technologies, which determines the relevance of their further research.

Special attention is paid to the study of noble metal nanoparticles, which exhibit well-known localized surface plasmon resonance (LSPR) [2, 5–7]. Among them, Ag nanoparticles (AgNPs) have unique optoelectronic properties, are non-toxic and chemically stable, which makes them promising for application in various fields including diagnostics and energy-saving technologies [8, 9]. AgNPs can be prepared by several methods using inorganic silver salts, such as chemical reduction, photochemical and electrochemical methods, and microwave processing [10–14].

In recent years, the attention was focused on the green synthesis methods of AgNPs [15–18]. These methods are alternative to the use of expensive and dangerous reagents. Combined with the biocompatibility of used materials, they contribute to the expansion of the application of such NPs. An environmentally friendly method of synthesis of bionanocomposites based on chitosan deserves an especial attention [19].

Chitosan (Ch) is attractive due to its abundance in nature, biocompatibility, biodegradability and non-toxicity [20]. Its useful property is the possibility of obtaining chitosan and composites based on it in various forms such as films, fibers, gels, resins, membranes and sponges [21]. Physico-chemical properties of chitosan are decisive for its practical application and directly depend on the solvents used [22, 23].

A number of studies demonstrated the effectiveness of combining AgNPs with collagen, cellulose and chitosan [24]. Combination of nanoparticles with polymers increases stability and dispersibility and can also stabilize the structure of metal NPs preventing their spontaneous aggregation [25]. In order to obtain new materials with specific properties, polymers should be modified to stabilize the structure of macromolecules and improve the required properties such as solubility and temperature stability [26]. A great number of works [27, 28] are devoted to clarifying the mechanisms of action and effectiveness of AgNPs and chitosan nanocomposites against the most common antibiotic-resistant clinical isolates.

Considering the significant interest to obtaining new materials, this study is focused on the modified and stable chitosan-based nanocomposites with a significant portion of silver nanoparticles prepared by the simple and environmentally friendly method.

2. Experimental

2.1. Sample preparation

Chitosan-AgNPs nanocomposites were synthesized by chemical reduction using the "green chemistry" approach (Fig. 1). The starting materials for the synthesis were silver nitrate ($AgNO_3$, 99%) and ecologically friendly reducing agents, namely chitosan (deacetylation degree of 91.6%) and ascorbic acid ($C_6H_8O_6$, 0.87 wt.%). Chitosan was used as a stabilizer, silver nitrate as a source of silver, ascorbic acid as a reducing agent and acetic acid (CH_3COOH, 10 wt.%) as a solvent, respectively. Thin films of chitosan-chitin (Ch-Chn) copolymer composites with different concentrations of Ag nanoparticles were prepared: Ch-Chn-9%AgNPs, Ch-Chn-15%AgNPs, Ch-Chn-22%AgNPs, Ch-Chn-34%AgNPs, Ch-Chn-50%AgNPs, Ch-Chn-71%AgNPs, and Ch-Chn-80%AgNPs.

2.2. Methods

The structure of the organic matrix in the prepared composite was investigated by Fourier-transform infrared spectroscopy (FTIR, Shimadzu IR Tracer-100 and Shimadzu FTIR-21 Prestige equipped with ATR-FTIR (ZnSe)). The AgNPs microstructure and distribution in the obtained composites were studied by scanning electron microscopy (SEM Vega Tescan 3 comprising secondary electron (SE) and backscattered-electron (BSE) detectors, applied accelerating voltage of 30 kV, working distance around 10 mm). The elemental composition of the samples was determined by using the scanning electron microscope (Tescan VEGA3) equipped with an energy dispersive X-ray detector (EDS) (Oxford Instruments). The UV-VIS spectral characteristics were studied by diffuse reflectance spectroscopy (Shimadzu UV-2600 UV–VIS spectrophotometer equipped with a photomultiplier and semiconductor InGaAs detectors, spectral range: 190…1400 nm, 1 nm scan step, UV Probe software operating an ISR-2600Plus integrating sphere).

3. Results and discussion

3.1. The organic matrix structure

The structure of the organic matrix of the prepared nanocomposites was determined analyzing the FTIR spectra of the Ag-free chitosan-based polymer film. FTIR spectra were recorded in the transmission (Shimadzu IR Tracer-100) and reflection (Shimadzu FTIR-21 Prestige) mode (see inset in Fig. 2).

The FTIR spectra of the obtained composites (see inset in Fig. 2) reveal characteristic vibrations of the groups corresponding to the polysaccharide structure of the original chitosan (marked red) and carboxyl groups (marked blue) of the acetic acid used to prepare the films. The FTIR spectra of the pure polymer film contain characteristic bands of polysaccharides corresponding to the deformation vibrations of C–H groups present in the structure of polysaccharides (943…897 cm^{-1}), asymmetric valence vibrations C–O–C of pyranose ring or –C–OH glycosidic hydroxyl (1150…1020 cm^{-1}), and valence vibrations of CH_2 groups (2926…2876 cm^{-1}). The bands corresponding to the valence vibrations of hydroxyl and the deformation vibrations of amino groups overlap in the spectral range of 3700…2950 cm^{-1} which leads to smoothening of the spectrum obtained in the transmission mode. Characteristic reflexes of carboxylic acids are observed in the spectral ranges of 1550…1412 and 1289…1258 cm^{-1}. A strong broad signal from the carboxyl group (1880…1800 cm^{-1}) is present in the spectrum obtained in the transmission mode. The presence of the two systems of reflexes may be related to the preparation of the chitosan-chitin copolymer film [26].

The FTIR spectra of the obtained chitosan and AgNPs composite films recorded in the transmission mode (Fig. 2) are characterized by absence of additional vibrations indicating no formation of new bonds. The intensities of the characteristic reflexes of the organic matrix significantly decrease with the gradual increase in the silver content. As a result, vibrational bands of the atomic groups appear only in the composites with the Ag^0 content of 9, 22, and 34 wt.% (Fig. 2). The decrease in the intensity of the reflexes is associated with the decrease in the amount of organic polymer in the nanocomposites from 91 to 21 wt.%.

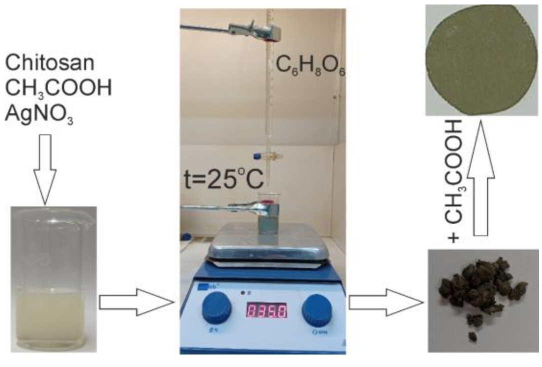

Fig. 1. Preparation scheme of nanocomposite thin films based on chitosan and AgNPs.

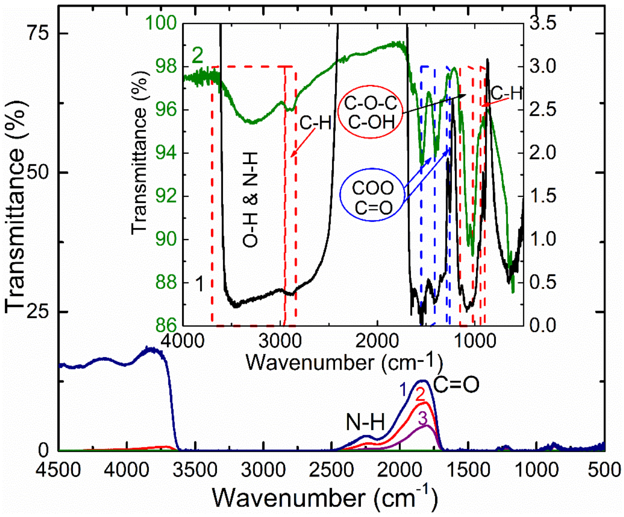

Fig. 2. FTIR spectra of the nanocomposite films based on chitosan and AgNPs (*1* – Ch-Chn-9%AgNPs, *2* – Ch-Chn-15%AgNPs, *3* – Ch-Chn-22%AgNPs). The inset shows FTIR spectra of a pure chitosan polymer film obtained in different modes (*1* – transmission and *2* – reflection).

3.2. Microstructure of composite films

Analysis of the SEM images (see inset in Fig. 3a) and EDS results (Fig. 3a) reveals uniform distribution of the silver nanoparticles in the chitin-chitosan composite and compliance with the content of Ag^0 in the composite provided in Fig. 3b. It was found out that spherical AgNPs are uniformly distributed in the nanocomposite films and separated from each other (see inset in Fig. 3a). Analysis of the SEM images for the exemplary cases of low (9% wt.% Ag) and high (71 wt.% Ag) silver content reveals noticeable aggregation of the AgNPs in the latter case. Elemental composition analysis (in atomic and weight %) shows presence of the carbon and oxygen peaks related to the organic matrix as well as the corresponding silver peaks.

The dependence of the theoretically calculated Ag concentration on the experimental one obtained by EDS analysis (Fig. 3b) is monotonous and almost linear. EDS analysis of the spectra of the nanocomposites in the Ag^0 concentration range from 9 to 50 wt.% shows a positive deviation from linearity (Fig. 3b), which may be attributed to sufficiently large distances between the silver nanoparticles in the composite. The content of Ag^0 in the samples with theoretically calculated values of 71…80 wt.% is smaller within the error of the method of ±1-2% (Fig. 3b). Such distribution of silver concentration in the composite is an indication of the aggregation phenomena. The proximity of the experimental and theoretical Ag^0 concentrations confirms complete reduction of $Ag^+ \rightarrow Ag^0$ in the direct process of composite preparation.

3.3. Optical properties

Diffuse reflectance spectroscopy is a simple and reliable method to study optical properties of powdery, crystalline, and nanostructured materials in various spectral ranges [29, 30]. When a material containing a significant number of particles (crystallites, nanoparticles) is irradiated, the incident radiation is focused on the sample and can be reflected in two ways, namely diffuse and specular. Two components of the incident beam energy are considered. One portion of the radiation penetrates through the sample and the other one is reflected from its surface in all directions. Diffuse reflection is the reflected radiation portion that returns to the sample surface and goes outside. Specular reflection is observed from a rough or uneven surface of the material and slightly contributes to the overall signal. Therefore, the reflection capture devices are optimized to maximize collecting of the diffuse reflection component and reduce the specular component [31]. Diffuse reflectance (R_d) is defined as the ratio of the intensity of the radiation reflected by the sample R_{sample} to the standard reflected intensity $R_{standard}$, corresponding to $BaSO_4$ in this case [29, 30].

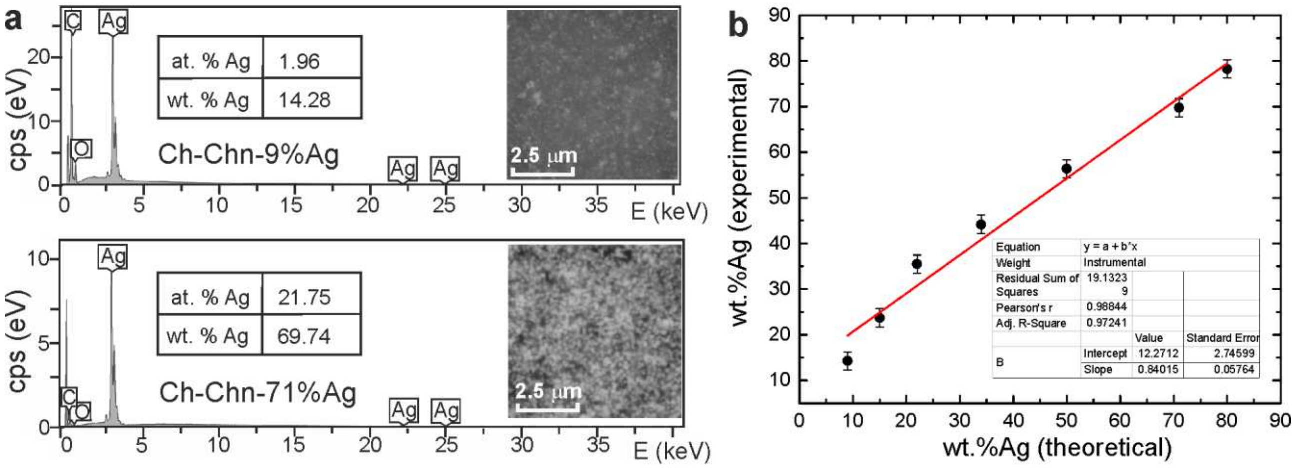

Fig. 3. EDS spectra and SEM images of the Ch-Chn-AgNPs composites (*a*), theoretically calculated *versus* experimentally obtained by EDS analysis concentrations of Ag (*b*).

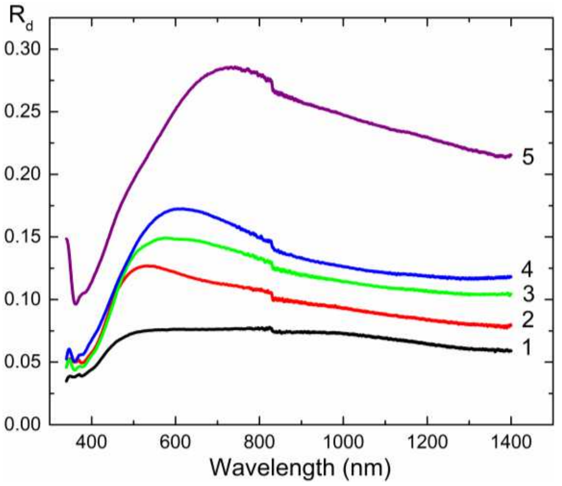

Fig. 4. Diffuse reflectance spectra of the Ch-Chn-AgNPs composites: *1* – Ch-Chn-9%AgNPs, *2* – Ch-Chn-22%AgNPs, *3* – Ch-Chn-34%AgNPs, *4* – Ch-Chn-50%AgNPs, *5* – Ch-Chn-71%AgNPs.

Diffuse reflectance spectra for the nanocomposite films with the AgNPs content in the range of 9…71 wt.% were obtained. Nanocomposite films were fabricated by dissolving the synthesized nanocomposites in a 10 wt.% acetic acid solution to form gel-like solutions. The resulting gels were deposited onto the substrates and dried in air (25 °C). As an outcome, thin films of chitosan-chitin copolymer with silver nanoparticles (Ch-Chn-AgNPs) on glass substrates were prepared. The diffuse reflectance spectra of these films relative to the spectrum of a pure chitosan film in the 350…1400 nm wavelength range were obtained. The recorded UV-VIS reflectance spectra are presented in Fig. 4.

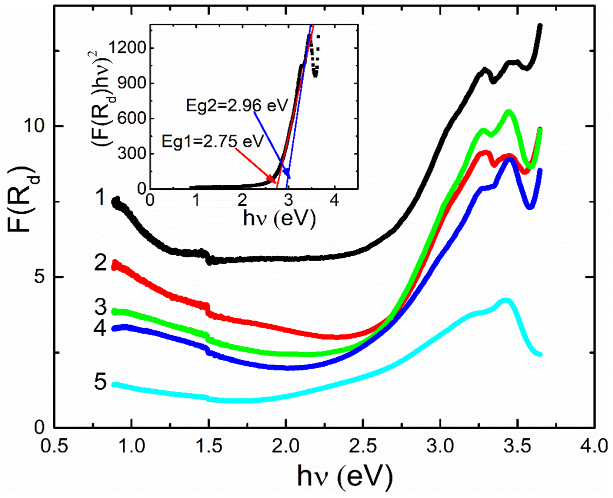

Fig. 5. Spectral dependences of the Kubelka–Munk function of the Ch-Chn-AgNPs composites: *1* – Ch-Chn-9%AgNPs, *2* – Ch-Chn-22%AgNPs, *3* – Ch-Chn-34%AgNPs, *4* – Ch-Chn-50%AgNPs, *5* – Ch-Chn-71%AgNPs. The inset shows the Tauc plot of the spectral dependence of the Kubelka–Munk function and the method of determination of the local plasmon E_{g1} and quadrupole E_{g2} resonance energies on the example of the Ch-Chn-AgNPs composite with 34% Ag concentration.

It was found out (Fig. 4) that the maximum positions on the diffuse reflectance spectra shifted from 498 to 733 nm with the increase in the Ag^0 concentration in the range from 9 to 71 wt.%. According to the Mie theory, the reflection maximum is related to LSPR of the AgNPs nanoparticles [32]. Moreover, an additional weak peak at 370 nm was revealed on the reflectance spectra, which corresponds to quadrupole plasmon resonance (Fig. 4) [33]. All the spectra of the studied nanocomposite samples also showed an effect at 829 nm, which was just a characteristic effect of switching the detectors in the Shimadzu UV-2600 device.

To estimate the optical transition energy values from the diffuse reflectance spectra, the Kubelka–Munk function, being one of the fundamental functions used for analyzing diffuse reflectance spectra of weakly absorbing materials [34, 35], should be used. In this case, the Kubelka–Munk function was used to convert the diffuse reflectance spectra into the absorption ones:

$$F[R_d(h\nu)] = \frac{[1-(R_d)h\nu]^2}{2R_d(h\nu)} \propto \frac{\alpha}{s} \propto \alpha ,$$

where R_d is the diffuse reflectance, α is the absorption coefficient, and s is the scattering coefficient, respectively. The latter parameter is constant at the sample thicknesses significantly exceeding the sizes of individual crystallites, in this case nanoparticles [30, 31] (Fig. 5).

As a result of the analysis of the spectral dependences of the Kubelka–Munk function for the nanocomposite films (Fig. 5), a monotonic shift of the absorption edge towards higher energies with the increase of the amount of Ag^0 was found. Detailed examination of the spectral dependences of the Kubelka–Munk function $F[R_d(h\nu)]$ revealed two linear segments becoming ever more distinct as the silver concentration in the composites decreased. This effect is related to the decrease of the nanoparticle size with lowering the silver concentration (Fig. 3).

It is well known that optical transitions in semiconductor materials may be direct and indirect. The value of the optical transition energy E_g can be calculated from the position of the main absorption peak corresponding to the electron transitions from the valence to the conduction band. For the detailed optical characterization of the silver nanoparticles by diffuse reflectance spectroscopy, the Kubelka–Munk function was used in combination with the Tauc method, which made possible to take into account the energy structure of the studied materials [7, 30, 31]:

$$F[R_d(h\nu)]^2 = A(h\nu - E_g) .$$

Here, E_g is the energy of the optical transition, A is the proportionality constant, and the power of 2 corresponds to the direct allowed optical transitions characteristic for noble metal nanoparticles [7].

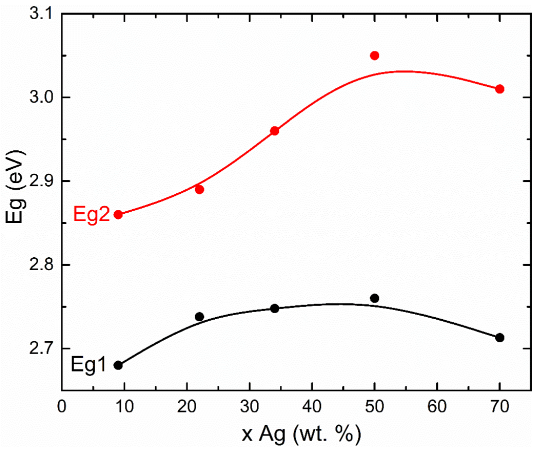

Fig. 6. Compositional dependences of the optical transition energies of local E_{g1} and quadrupole E_{g2} plasmon resonances on the size of the AgNPs.

The inset in Fig. 5 shows the Tauc plot of the spectral dependence of the Kubelka–Munk function and an example of determining the local plasmon (E_{g1}) and quadrupole (E_{g2}) resonance energies for the Ch-Chn-AgNPs composite with 34% Ag content. Combining the Kubelka–Munk function (to convert the diffuse reflectance spectrum into the absorption one) with the Tauc method (to take into account the energy structure) and using multilevel approximation by the least squares method, the energies E_{g1} and Eg_2 for the nanocomposites based on chitosan and AgNPs as functions of composition were determined (Fig. 6). The compositional dependences of E_{g1} and E_{g2} are nonlinear functions with maximum values at the Ag^0 concentration of 50 wt.% (E_{g1} = 2.76 eV and E_{g2} = 3.08 eV). Further increase in the Ag^0 content in the composite leads to a gradual decrease of the energies of optical transitions. These energies become E_{g1} = 2.71 eV and E_{g2} = 3.02 eV at the Ag^0 content of 71 wt.%. Such decrease may be attributed to the decrease in the distances between the Ag^0 particles in the composite resulted from aggregation, which will further lead to the transition from nano- to microsizes (Fig. 3).

4. Conclusions

Physical and chemical characteristics of chitosan polymer-based composites with silver nanoparticles were studied. The study was mainly focused on the chitosan-based system with silver nanoparticles (AgNPs). The formation of a chitin-chitosan copolymer film was detected using ATR–FTIR. The presence of the characteristic functional groups of polysaccharides in the nanocomposite films was confirmed by ATR–FTIR. According to the Mie theory, the maximum of absorption is related to LSPR of the AgNPs nanoparticles.

Diffuse reflectance spectra showed an additional weak reflectance peak around 370 nm corresponding to quadrupole plasmon resonance. The values of the energies of optical transitions in the nanocomposite samples were determined from the study of electron absorption and transitions using the Kubelka–Munk function and the Tauc plots. As a result, the energy values of the optical transitions of local (E_{g1}) and quadrupole (E_{g2}) plasmon resonances were obtained.

Based on the above-mentioned results, the compositional dependences of E_{g1} and E_{g2} in the Ch-Chn-AgNPs nanocomposites were constructed. These dependences are nonlinear with the maxima at the Ag^0 concentration of 50 wt.% (E_{g1} = 2.76 eV та E_{g2} = 3.08 eV).

Acknowledgements

The work at the P.J. Šafarik University was supported by the grant of the Slovak Research and Development Agency under the contract APVV-20-0324 and by the National Scholarship Programme of the Slovak Republic [Grant ID 39133].

The authors would also like to thank the Armed Forces of Ukraine for providing security to perform this work. This work has become possible only because of the resilience and courage of the Ukrainian Army.

References

1. Sanjay M.R., Parameswaranpillai J., Yashas Gowda T.G., Siengchin S., Seydibeyoglu M.O. (Eds). *Nanoparticle-Based Polymer Composites*. Elsevier, Cambridge, Kidlington, 2022. https://doi.org/10.1016/C2020-0-01662-2.
2. Khan I., Saeed K., Khan I. Nanoparticles: Properties, applications and toxicities. *Arab. J. Chem.* 2019. **12**, No 7. P. 908–931. https://doi.org/10.1016/j.arabjc.2017.05.011.
3. Khodashenas B., Ghorbani H.R. Synthesis of silver nanoparticles with different shapes. *Arab. J. Chem.* 2019. **12**, No 8. P. 1823–1838. https://doi.org/10.1016/j.arabjc.2014.12.014.
4. Shkir M., Yahia I.S., Kilany M. *et al.* Facile nanorods synthesis of KI:HAp and their structure-morphology, vibrational and bioactivity analyses for biomedical applications. *Ceram. Int.* 2019. **45**, No 1. P. 50–55. https://doi.org/10.1016/j.ceramint.2018.09.132.
5. Abdel-Aziz M.S., Shaheen M.S., El-Nekeety A.A., Abdel-Wahhab M.A. Antioxidant and antibacterial activity of silver nanoparticles biosynthesized using *Chenopodium murale* leaf extract. *J. Saudi Chem. Soc*. 2014. **18**, No 4. P. 356–363. https://doi.org/10.1016/j.jscs.2013.09.011.
6. Joudeh N., Linke D. Nanoparticle classification, physicochemical properties, characterization, and applications: a comprehensive review for biologists. *J. Nanobiotechnol.* 2022. **20**, No 1. P. 1–29. https://doi.org/10.1186/s12951-022-01477-8.
7. Meikhail M.S., Abdelghany A.M., Aldhabi A.A. Preparation and characterization of silver and gold nanoparticles and study influence on physical properties of PVA/PVP nanocomposites. *J. Adv. Phys*. 2017. **13**, No 1. P. 4628–4639. https://doi.org/10.24297/jap.v13i1.5626.

8. Shao W., Li G., Zhu P. *et al*. Facile synthesis of low temperature sintering Ag nanopaticles for printed flexible electronics. *J. Mater. Sci.: Mater. Electron*. 2018. **29**, No 6. P. 4432–4440. https://doi.org/10.1007/s10854-017-8390-4.
9. Alkhalayfeh M.A., Aziz A.A., Pakhuruddin M.Z., Katubi K.M.M. Plasmonic effects of Au@Ag nanoparticles in buffer and active layers of polymer solar cells for efficiency enhancement. *Materials*. 2022. **15**, No 16. P. 5472. https://doi.org/10.3390/ma15165472.
10. Gharibshahi L., Saion E., Gharibshahi E. *et al*. Structural and optical properties of Ag nanoparticles synthesized by thermal treatment method. *Materials*. 2017. **10**, No 4. P. 402. https://doi.org/10.3390/ma10040402.
11. Quintero-Quiroz C., Acevedo N., Zapata-Giraldo J. *et al*. Optimization of silver nanoparticle synthesis by chemical reduction and evaluation of its antimicrobial and toxic activity. *Biomater. Res*. 2020. **23**, No 1. P. 1–15. https://doi.org/10.1186/s40824-019-0173-y.
12. Huang M., Du L., Feng J.X. Photochemical synthesis of silver nanoparticles/eggshell membrane composite, its characterization and antibacterial activity. *Sci. Adv. Mater*. 2016. **8**, No 8. P. 1641–1647. https://doi.org/10.1166/sam.2016.2777.
13. Kuntyi O., Mazur A., Kytsya A. *et al*. Electrochemical synthesis of silver nanoparticles in solutions of rhamnolipid. *Micro & Nano Lett*. 2020. **15**, No 12. P. 802–807. https://doi.org/10.1049/mnl.2020.0195.
14. Seku K., Gangapuram B.R., Pejjai B. *et al*. Microwave-assisted synthesis of silver nanoparticles and their application in catalytic, antibacterial and antioxidant activities. *J. Nanostructure Chem*. 2018. **8**, No 2. P. 179–188. https://doi.org/10.1007/s40097-018-0264-7.
15. Nouri A., Yaraki M.T., Lajevardi A., Rezaei Z., Ghorbanpour M., Tanzifi M. Ultrasonic-assisted green synthesis of silver nanoparticles using Mentha aquatica leaf extract for enhanced antibacterial properties and catalytic activity. *Colloid Interface Sci. Commun*. 2020. **35**. P. 100252. https://doi.org/10.1016/j.colcom.2020.100252.
16. Fizer M.M., Mariychuk R.T., Fizer O.I. Gold nanoparticles green synthesis with clove oil: spectroscopic and theoretical study. *Appl. Nanosci*. 2022. **12**, No 3. P. 611–620. https://doi.org/10.1007/s13204-021-01726-6.
17. Widatalla H.A., Yassin L.F., Alrasheid A.A. *et al*. Green synthesis of silver nanoparticles using green tea leaf extract, characterization and evaluation of antimicrobial activity. *Nanoscale Adv*. 2022. **4**, No 3. P. 911–915. https://doi.org/10.1039/D1NA00509J.
18. Alharbi N.S., Alsubhi N.S., Felimban A.I. Green synthesis of silver nanoparticles using medicinal plants: Characterization and application. *J. Radiat. Res. Appl. Sci*. 2022. **15**, No 3. P. 109–124. https://doi.org/10.1016/j.jrras.2022.06.012.
19. Bashir S.M., Rather G.A., Patrício A. *et al*. Chitosan nanoparticles: A versatile platform for biomedical applications. *Mater*. 2022. **15**, No 19. P. 6521. https://doi.org/10.3390/ma15196521.
20. Shariatinia Z. Pharmaceutical applications of chitosan. *Adv. Colloid Interface Sci*. 2019. **263**. P. 131–194. https://doi.org/10.1016/j.cis.2018.11.008.
21. El-hefian E.A., Nasef M., Yahaya A. Chitosan physical forms: a short review. *Australian Journal of Basic and Applied Sciences*. 2011. **5**. P. 670–677.
22. Sacco P., Furlani F., De Marzo G. *et al*. Concepts for developing physical gels of chitosan and of chitosan derivatives. *Gels*. 2018. **4**, No 3. P. 67. https://doi.org/10.3390/gels4030067.
23. Essel T.Y., Koomson A., Seniagya M.P.O. *et al*. Chitosan composites synthesized using acetic acid and tetraethylorthosilicate respond differently to methylene blue adsorption. *Polymers*. 2018. **10**, No 5. P. 466. https://doi.org/10.3390/polym10050466.
24. Pocoví-Martínez S., Cassano D., Voliani V. Naked nanoparticles in silica nanocapsules: a versatile family of nanorattle catalysts. *ACS Appl. Nano Mater*. 2018. **1**, No 4. P. 1836–1840. https://doi.org/10.1021/acsanm.8b00247.
25. Bankier C., Matharu R.K., Cheong Y.K. *et al*. Synergistic antibacterial effects of metallic nanoparticle combinations. *Sci. Rep*. 2019. **9**, No 1. P. 1–8. https://doi.org/10.1038/s41598-019-52473-2.
26. Argüelles-Monal W.M., Lizardi-Mendoza J., Fernández-Quiroz D. *et al*. Chitosan derivatives: Introducing new functionalities with a controlled molecular architecture for innovative materials. *Polymers*. 2018. **10**, No 3. P. 342. https://doi.org/10.3390/polym10030342.
27. Shariatinia Z. Pharmaceutical applications of chitosan. *Adv.Colloid Interface Sci*. 2019. **263**. P. 131–194. https://doi.org/10.1016/j.cis.2018.11.008.
28. Abedian Z., Jenabian N., Moghadamnia A.A. *et al*. Antibacterial activity of high-molecular-weight and low-molecular-weight chitosan upon oral pathogens. *J. Conserv. Dent*. 2019. **22**, No 2. P. 169–174. https://doi.org/10.4103/JCD.JCD_300_18.
29. Pogodin A.I., Malakhovska T.O., Filep M.J. *et al*. Optical pseudogap of $Ag_7(Si_{1-x}Ge_x)S_5I$ solid solutions. *Ukr. J. Phys. Opt*. 2022. **23**, No 2. P. 77–85. https://doi.org/10.3116/16091833/23/2/77/2022.
30. Pogodin A.I., Filep M.J., Malakhovska T.O. *et al*. Microstructural, mechanical and electrical properties of superionic $Ag_{6+x}(P_{1-x}Ge_x)S_5I$ ceramic materials. *J. Phys. Chem. Solids*. 2022. **171**. P. 111042. https://doi.org/10.1016/j.jpcs.2022.111042.
31. Aydın C., Abd El-sadek M.S., Zheng K., Yahia I.S., Yakuphanoglu F. Synthesis, diffused reflectance and electrical properties of nanocrystalline Fe-doped ZnO via sol–gel calcination technique. *Opt. Laser Technol.* 2013. **48**. P. 447–452. https://doi.org/10.1016/j.optlastec.2012.11.004.

32. Hong E.J., Kim Y.S., Choi D.G., Shim M.S. Cancer-targeted photothermal therapy using aptamer-conjugated gold nanoparticles. *J. Indust. Eng. Chem.* 2018. **67**. P. 429–436. https://doi.org/10.1016/j.jiec.2018.07.017.
33. Amirjani A., Koochak N.N., Haghshenas D.F. Synthesis of silver nanotriangles with tunable edge length: A promising candidate for light harvesting purposes within visible and near–infrared ranges. *Mater. Res. Exp*. 2018. **6**, No 3. P. 036204. https://doi.org/10.1088/2053-1591/aaf624.
34. Yang L, Kruse B. Revised Kubelka–Munk theory. I. Theory and application. *J. Opt. Soc. Am. A*. 2004. **21**. P. 1933–1941. https://doi.org/10.1364/JOSAA.21.001933.
35. Yakuphanoglu F., Mehrotra R., Gupta A., Munoz M. Nanofiber organic semiconductors: The effects of nanosize on the electrical charge transport and optical properties of bulk polyanilines. *J. Appl. Polym. Sci*. 2009. **114**. P. 794–799. https://doi.org/10.1002/app.28535.

Authors and CV

Tetyana O. Malakhovska, born in 1983, defended her PhD thesis in inorganic chemistry in 2010. Senior researcher at the Uzhhorod National University. Authored 70 articles and 10 patents. The area of her scientific interests includes solid state chemistry and materials science. E-mail: t.malakhovska@gmail.com, https://orcid.org/0000-0001-7309-4894

Artem I. Pogodin, defended his PhD thesis in Inorganic Chemistry in 2016. Senior Researcher at the Uzhhorod National University. Authored over 100 scientific articles and 100 patents. The area of his scientific interests includes solid state chemistry, crystal growth and materials science. E-mail: artempogodin88@gmail.com, https://orcid.org/0000-0002-2430-3220

Mykhailo J. Filep, born in 1987, defended his PhD thesis in Inorganic Chemistry in 2015. Senior Researcher at the Uzhhorod National University. Authored over 100 articles and 50 patents. The area of his scientific interests includes solid state chemistry and materials science. E-mail: mfilep23@gmail.com, http://orcid.org/0000-0001-7017-5437

Mykhailo M. Pop, born in 1982, defended his PhD thesis in Physics and Mathematics in 2016. Lecturer and Researcher at the Uzhhorod National University. Authored nearly 100 publications. The area of his scientific interests includes physical and optical properties of semiconductors, superionic materials, chalcogenide glasses and films. E-mail: mykhaylo.pop@uzhnu.edu.ua, https://orcid.org/0000-0003-3674-3482

Yaroslav Studenyak, PhD, Associate Professor at the Department of Analytical Chemistry, Uzhhorod National University. Author of over 20 publications indexed in the Scopus and Web of Science databases as well as 9 patents. E-mail: yaroslav.studenyak@uzhnu.edu.ua https://orcid.org/0000-0002-8970-2222

Kateryna Nemesh, born in 2000. Master student at the Educational and Scientific Institute of Chemistry and Ecology of the Uzhhorod National University and the Faculty of Chemistry of the Pavel Jozef Šafárik University in Košice. The area of her scientific interests includes electrical properties of superionic conductors and thermal methods of analysis. E-mail: katya.nemesh2000@gmail.com, https://orcid.org/0000-0001-6375-1627

Ruslan Mariychuk, PhD, Associate Professor at the Department of Ecology, University of Presov, Presov, Slovakia. Author of over 60 publications indexed in the Scopus and Web of Science databases as well as 3 patents. His research interests include green chemistry, sustainable synthesis of nanomaterials and materials science. E-mail: ruslan.mariychuk@unipo.sk, https://orcid.org/0000-0001-8464-4142

Vasyl V. Vakulchak, born in 1986, defended his PhD thesis in Physics and Mathematics in 2015. Senior Researcher of the Department of Applied Physics at the Uzhhorod National University. Authored over 80 publications and 1 patent. The area of his scientific interests includes *ab-initio* calculations of electronic structure and physical properties of semiconductors. E-mail: vasyl.vakulchak@uzhnu.edu.ua, https://orcid.org/0000-0001-6037-8978

Vladimir Komanicky, born in 1974, defended his PhD thesis in Chemistry in 2003 at the University of California. Leading Scientist in the Electrocatalysis and Nanotechnology group at the Institute of Physics of the Pavol Jozef Safarik University in Kosice. Author of 107 publications, 2 patents and two textbooks. The area of his scientific interests includes nanotechnology, electrocatalysis, semiconductor physics, magnetism and superconductivity.
E-mail: vladimir.komanicky@upjs.sk,
https://orcid.org/0000-0001-8649-1987

Serhii Vorobiov, born in 1988, defended his PhD thesis in Physics and Mathematics at the Sumy State University, Ukraine in 2015. Postdoctoral Researcher at the Institute of Physics, Faculty of Science, Pavol Jozef Safarik University, Slovakia. Author of 46 publications indexed in the Scopus and Web of Science databases as well as 1 patent. The area of his scientific interests includes nanofabrication and thin film technology, magnetic and magnetoresistance properties of nano- and mesoscopic systems. E-mail: serhii.vorobiov@upjs.sk,
https://orcid.org/0000-0002-5884-3292

Authors' contributions

Malakhovska T.O.: supervision, conceptualization, investigation, writing – original draft.
Pogodin A.I.: investigation, writing – original draft, visualization, validation.
Filep M.J.: investigation, writing – original draft.
Pop M.M.: investigation, writing – review & editing.
Studenyak Ya.I.: methodology, visualization.
Nemesh K.M.: investigation.
Mariychuk R.: writing – review & editing.
Vakulchak V.V.: investigation, visualization.
Komanicky V.: methodology, writing – review & editing.
Vorobiov S.: methodology, visualization.

Оптичні характеристики нанокомпозитів на основі срібла, одержані екологічно чистим методом

Т.О. Малаховська, А.І. Погодін, М.Й. Філеп, М.М. Поп, Я.І. Студеняк, К.М. Немеш, Р. Марійчук, В.В. Вакульчак, В. Команіцкі, С. Воробйов

Анотація. У цій роботі представлено простий та екологічно безпечний метод синтезу нанокомпозитів на основі хітозану та Ag. Структуру отриманої органічної матриці встановлено методом інфрачервоної FTIR спектроскопії. Установлено утворення сополімеру хітозан-хітин. Одержано нанокомпозитні плівки з вмістом срібла 9–71 мас.%. Методами скануючої електронної мікроскопії та енергодисперсійної рентгенівської спектроскопії досліджено мікроструктуру та елементний аналіз отриманих плівок. Отримані плівки характеризуються рівномірним розподілом наночастинок срібла в органічній матриці. Оптичні властивості досліджували методом спектроскопії дифузного відбиття. Спектри дифузного відбиття плівок характеризуються наявністю максимуму. Встановлено, що збільшення концентрації Ag^0 у нанокомпозитних плівках приводить до зміщення максимуму на спектрах дифузного відбиття у більш довгохвильовий діапазон хвиль. За допомогою функції Кубелки–Мунка у поєднанні з методом Таука визначено енергії оптичних переходів.

Ключові слова: хітозан, наночастинки, композити, скануюча електронна мікроскопія, спектроскопія дифузного відбиття.